

Metatranscriptomic insights into host-microbiome interactions underlying asymptomatic COVID-19 cases

Received: 25 August 2025

Accepted: 13 February 2026

Published online: 03 March 2026

Cite this article as: Chowdhury S.F., Sarkar M.M.H., Al Sium S.M. *et al.* Metatranscriptomic insights into host-microbiome interactions underlying asymptomatic COVID-19 cases. *Sci Rep* (2026). <https://doi.org/10.1038/s41598-026-40563-x>

Sanjana Fatema Chowdhury, Md. Murshed Hasan Sarkar, Syed Muktadir Al Sium, Showti Raheel Naser, Md. Saddam Hossain, Md. Ahashan Habib, Shahina Akter, Tanjina Akhtar Banu, Barna Goswami, Iffat Jahan, Tanay Chakrovarty, M. Maruf Ahmed Molla, Tasnim Nafisa, Mahmuda Yeasmin, Asish Kumar Ghosh & Md. Salim Khan

We are providing an unedited version of this manuscript to give early access to its findings. Before final publication, the manuscript will undergo further editing. Please note there may be errors present which affect the content, and all legal disclaimers apply.

If this paper is publishing under a Transparent Peer Review model then Peer Review reports will publish with the final article.

Metatranscriptomic Insights into Host-Microbiome Interactions Underlying Asymptomatic COVID-19 Cases

Sanjana Fatema Chowdhury¹, Md. Murshed Hasan Sarkar^{1*}, Syed Muktedir Al Sium¹, Showti Raheel Naser¹, Md. Saddam Hossain¹, Md. Ahashan Habib¹, Shahina Akter¹, Tanjina Akhtar Banu¹, Barna Goswami¹, Iffat Jahan¹, Tanay Chakrovarty^{1,2}, Md. Maruf Ahmed Molla³, Tasnim Nafisa³, Mahmuda Yeasmin³, Asish Kumar Ghosh³, Md. Salim Khan^{1*}

1. Bangladesh Council of Scientific and Industrial Research (BCSIR), Dhaka -1205, Bangladesh

2. Jashore University of Science and Technology (JUST), Jashore, Bangladesh

3. National Institute of Laboratory Medicine & Referral Center (NILMRC), Dhaka, Bangladesh

Corresponding address:

Md. Murshed Hasan Sarkar - murshed_mbdu@yahoo.com

Md. Salim Khan - k2salim@yahoo.com

Abstract:

Coronavirus disease 2019 (COVID-19) remains a major global health concern, with emerging evidence highlighting the role of the human microbiome in influencing disease severity. While extensive research has been conducted on COVID-19, studies examining host-pathogen interactions at the transcriptomic level remain limited. In this study, we investigated the metatranscriptomic profiles of forty nasopharyngeal samples collected from COVID-19 patients across different Bangladeshi cohorts. Sequencing data were processed to analyze taxonomic composition, microbial diversity, and antimicrobial resistance gene (ARG) patterns using multiple bioinformatic pipelines. COVID-19 positive and asymptomatic patients exhibited a higher abundance of pathogenic and multidrug-resistant bacteria, whereas COVID-19 negative individuals showed increased fungal diversity. Differential gene expression analysis revealed significant upregulation of immune response related genes, including pro-inflammatory cytokines, in COVID-19 positive cases. Notably, asymptomatic patients demonstrated reduced TLR4 expression, suggesting a potential reducing of innate immune activation, which may contribute to asymptomatic clinical outcomes. Additionally, functional enrichment highlighted active ARG expression in positive cases, indicating potential links between the respiratory microbiome and host immune modulation. These findings provide insights into the host-microbiome interplay underlying COVID-19 severity and highlight the need for further validation in larger, ethnically diverse cohorts with comprehensive clinical metadata.

Keywords: COVID-19, Metatranscriptomics, Immunological signaling, Differential gene expression, Transcriptome

42 **Introduction**

43 Severe acute respiratory syndrome coronavirus 2 (SARS-CoV-2), the causative agent of
44 coronavirus disease 2019 (COVID-19), has created a catastrophic event throughout the world
45 known as COVID-19 pandemic [1,2]. The first cluster of COVID-19 cases was identified in
46 Wuhan, China, in late December 2019, where patients presented with symptoms of severe
47 pneumonia. Since then, SARS-CoV-2 has been considered as one of the deadliest human
48 pathogens after Spanish Flu [3,4]. However, fatality and prognosis of COVID-19 are influenced
49 by several factors such as patients' age or preexisting comorbidities (diabetes, hypertension,
50 asthma etc.) [5,6]. Vaccines have made it possible to reduce the severity of the disease, but
51 emergence of such viral disease still remains a threat. Since the COVID-19 outbreak, there has
52 been a significant increase in the collection of epidemiological, clinical, and immunological data.
53 But the molecular mechanism underlying SARS-CoV-2 virus pathogenesis and prognosis was still
54 not explored much [7,8]. This is because a thorough understanding of the pathogenesis of COVID-
55 19 should enable the development of effective strategies to enhance the generation of effective
56 anti-SARS-CoV-2 immune responses.

57 The respiratory microbiota consists of a wide range of bacteria and is distributed in the upper
58 respiratory tract (URT). This microbial flora contains either commensals or pathobionts. Various
59 investigations have shown that the severity of SARS-CoV-2 infection is likely to be influenced by
60 the co-existing bacteria, fungi, and archaea in the respiratory tracts [9,10]. The SARS-CoV-2 virus
61 enters the body by inhalation and binds to epithelial cells in the nasal cavity. It then replicates and
62 migrates through the respiratory tract and gradually proceeds towards the lungs to initiate infection
63 which in turn mounts a vigorous innate immune response for clearing up the virus [11]. So, it is
64 believed that during this propagation and immune response, the microbiota residing in the
65 respiratory airways may be altered, and inclusion of some of the pathobionts might alleviate the
66 course and severity of the disease caused by SARS-CoV-2 virus [11].

67 Nowadays, Next-generation sequencing (NGS) approaches, such as metagenomics, is the widely
68 used method for analyzing what kind of microbial population is present in a sample. But
69 metagenomics mainly focuses on the genomic content and identification of microbes present
70 within a community, while metatranscriptomics provides the diversity of the active genes within
71 such community, their expression level profile and how these levels change with alterations in
72 environmental conditions. Thus, to understand the role of respiratory microbiome in COVID-19
73 severity and to elucidate host gene expression with functional profiling metatranscriptomics
74 approaches are preferable.

75 In this study, nasopharyngeal samples of different severity groups of COVID-19 patients were
76 collected and subjected to sequencing to analyze both respiratory microbiome and differential gene
77 expression and immunological signaling pathways of the host [12,13]. This information not only
78 can be used for taxonomic characterization of known or novel microbes and host response analysis
79 but also determines the functional profile of biological processes of normal and altered respiratory
80 microbiome [13,14].

81

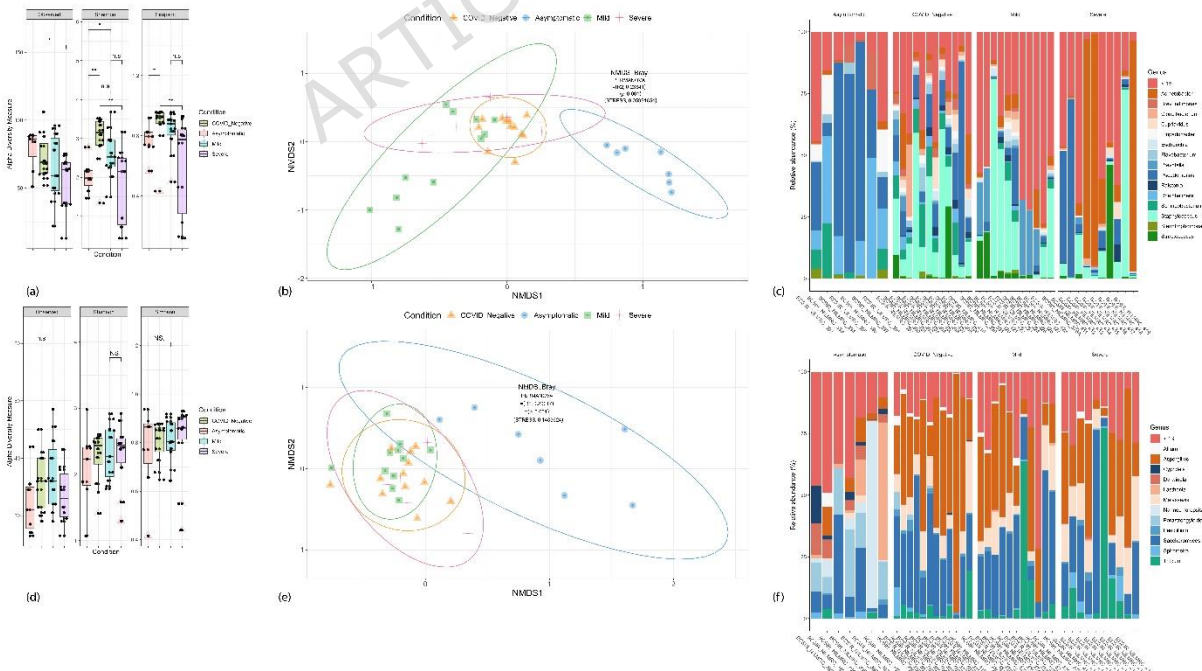
82 **Results:**83 **Taxonomic and microbial diversity analysis:**

84 Sequencing yielded an average of 3.1 million paired-end reads per sample. Read distribution
 85 analysis revealed consistent coverage across coding regions in all samples, with comparable
 86 representation of 5'UTR and 3'UTR segments (S2). No sample showed a dominant accumulation
 87 of reads at the 3' end or a depletion of 5' transcript regions, indicating the absence of strong 5'–3'
 88 degradation bias. The observed mild positional variation is consistent with expected Illumina
 89 RNA-seq library characteristics [15]. Ribosomal RNA depletion efficiency analysis showed only
 90 a small fraction of reads mapped to rRNA features (<0.5%, with a mean of $0.14\% \pm 0.10\%$),
 91 confirming effective depletion and high-quality library preparation. The percentage of rRNA
 92 across the samples is plotted in a barplot (S2).

93 Alignment to the human genome revealed that approximately 44% of these reads were of human
 94 origin, while the remaining 56% corresponded to microbial sequences. These microbial reads were
 95 subsequently used for all taxonomic analyses.

96 Alpha diversity measured using Shannon and Simpson Diversity metrics showed significant
 97 species diversity within the sample groups in terms of prokaryotes (Fig 1a). But in terms of
 98 Eukaryotes, the box and whisker plot show widespread distribution of species diversity for the
 99 severe group, whereas for the other three groups, the data were clustered (Fig 1d).

100 However, Bray–Curtis distance method Beta diversity analysis showed a separate cluster for
 101 Asymptomatic group in PCoA but the clusters of other three sample groups (Negative, Mild,
 102 Severe) overlapped for both the prokaryotes and eukaryotes (Fig 1b, 1e).



104 Fig 1: Alpha (a) and Beta (b) diversity indexes in Prokaryotes. Alpha (d) and Beta (e) diversity
105 indexes in Eukaryotes. Genus level Relative abundance of four major study cohorts. Here, (c)
106 Prokaryotes and (f) Eukaryotes.

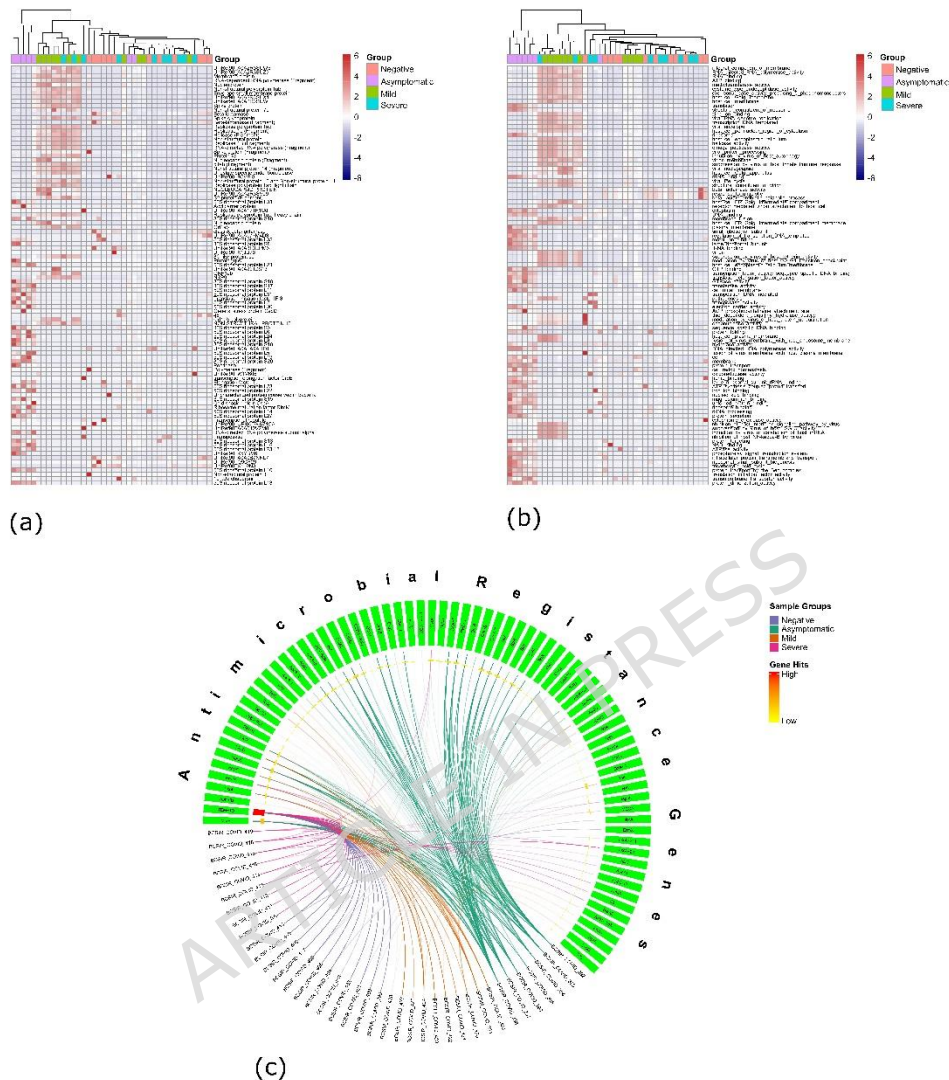
107

108 The relative abundance analysis across the four major study groups suggested a higher presence
109 of potentially pathogenic and multidrug-resistant bacterial strains among COVID-19 positive
110 patients, regardless of disease severity (Fig. 1c, 1f). Additionally, COVID-19 positive samples
111 appeared to show an increased fungal representation alongside SARS-CoV-2 infection.

112 **Microbial metatranscriptomics and antimicrobial resistance** 113 **analysis:**

114 The diversity in microbial community delved into looking more closely at the condition of
115 microbial metatranscriptomics in the samples. This analysis reveals the functions of microbial
116 communities by checking the transcriptome of the microbiome in each environment.

ARTICLE IN PRESS



117
 118 Fig 2: Here, (a) showing Gene Family abundance and (b) showing GO Term abundance in all the
 119 samples. Also, (c) showing a circos plot analysis of antibiotic resistance in asymptomatic positive
 120 patients visualizing the presence of different AMR genes across the isolates. A heatmap in the
 121 inner circle of the plot illustrates the frequency of each AMR gene across all isolates, with red
 122 indicating high frequency and yellow indicating low frequency.

123
 124 Differences in gene expression patterns and functional activity were observed in different study
 125 cohorts of COVID-19 patients in terms of severity. Substantial up-regulation of translation
 126 machinery and ribosomal proteins, including multiple 50S and 30S ribosomal proteins, was
 127 observed in the microbial gene expression profile of asymptomatic patients (Fig 2a). Along with
 128 that, genes linked to porins, and cold shock proteins were also highly expressed. Moreover, Gene
 129 Ontology (GO) analysis revealed enrichment in molecular functions including DNA binding,

130 GTPase activity, and magnesium ion binding, as well as biological processes like translation
131 elongation, protein transport, and the tricarboxylic acid cycle (Fig 2b).

132 Significant up-regulation of viral genes, such as replicase polyprotein 1AB, spike glycoprotein,
133 and RNA-directed RNA polymerase, was observed in mild COVID-19 patients. The structural
134 components of virions, host immune response regulation, and processes related to the viral life
135 cycle were found to have enrichment, according to GO analysis.

136 Stress response proteins, such as Rubredoxin and class D beta-lactamase, were up-regulated in the
137 microbial gene expression profile of severe COVID-19 patients. GO analysis showed inhibition of
138 the host antiviral signal, modification of host protein ubiquitination, and enrichment in processes
139 associated with the viral life cycle.

140 Genes related to beta-lactamase activity, cytochrome C oxidase activity, and aerobic respiration
141 were all overexpressed in the negative group. GO enrichment reflected normal cellular activity in
142 the absence of severe viral infection and was linked to host immunological suppression by viral
143 processes, sensitivity to drugs, and mitochondrial function.

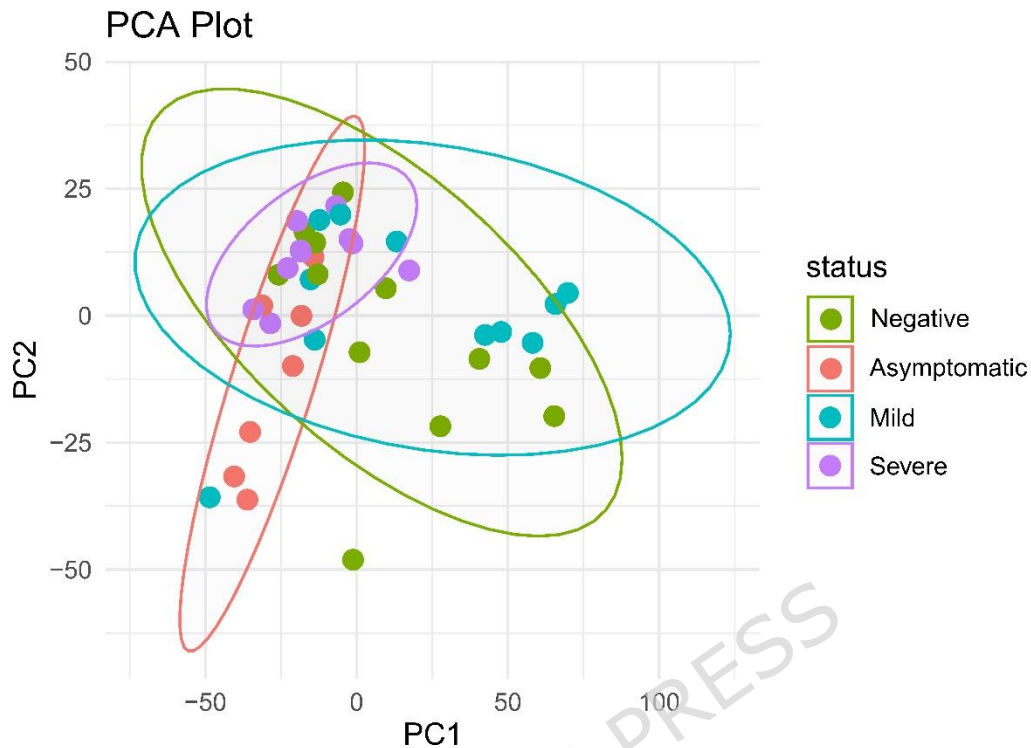
144 Analysis of antimicrobial resistance gene (ARG) profiles across the study cohorts revealed a
145 markedly higher abundance and diversity of ARGs in the asymptomatic COVID-19 group
146 compared to mild, severe, and negative cohorts. The asymptomatic COVID-19 cohort harbored a
147 distinct resistome, enriched in genes conferring resistance to aminoglycosides, trimethoprim,
148 phenicols, and rifamycins, which were largely absent in other severity groups. However, the β -
149 lactamase gene *TEM1-D* was present across all cohorts and highlighted in red in the circos plot to
150 denote its high abundance (Fig 2c).

151 To further explore the functional activity of the microbiome's resistome, a differential abundance
152 analysis of ARGs was performed. This analysis revealed a distinct and statistically significant
153 upregulation of multiple ARGs in the asymptomatic cohort compared to symptomatic (mild and
154 severe) patients. In total, 22 ARGs were found to be significantly more abundant in asymptomatic
155 individuals (*adjusted p* < 0.05; Supplementary File S2). Notably, the most upregulated genes
156 included those conferring resistance to catalases (*CATA2*; $\log_2FC = 9.32$, *p* adj = 1.73×10^{-4}) and
157 macrolides (*MSRE*; $\log_2FC = 8.79$, *p* adj = 3.82×10^{-5} ; *MPHE*; $\log_2FC = 8.50$, *p* adj = 1.37×10^{-3}).
158 Additionally, genes conferring resistance to β -lactams (*PER-1*; $\log_2FC = 8.26$), sulfonamides
159 (*SULII*; $\log_2FC = 8.13$), and aminoglycosides (*STRA*, *STRB*) were also highly expressed in the
160 asymptomatic group.

161 **COVID-19 associated host gene expression and gene enrichment:**

162 The different transcriptional patterns of the Severe, Mild, Negative, and Asymptomatic groups
163 may be clearly seen in the PCA plot (Fig 3). The biological significance of the transcriptome
164 variations is shown by the clustering patterns and confidence ellipses, which show the variability
165 within groups and the gap between them. Host gene expression analysis results were further plotted
166 on different groups for better understanding of the outcomes. The detailed \log_2Fc value along with
167 adjusted P value is available in Supplementary file S3.

168

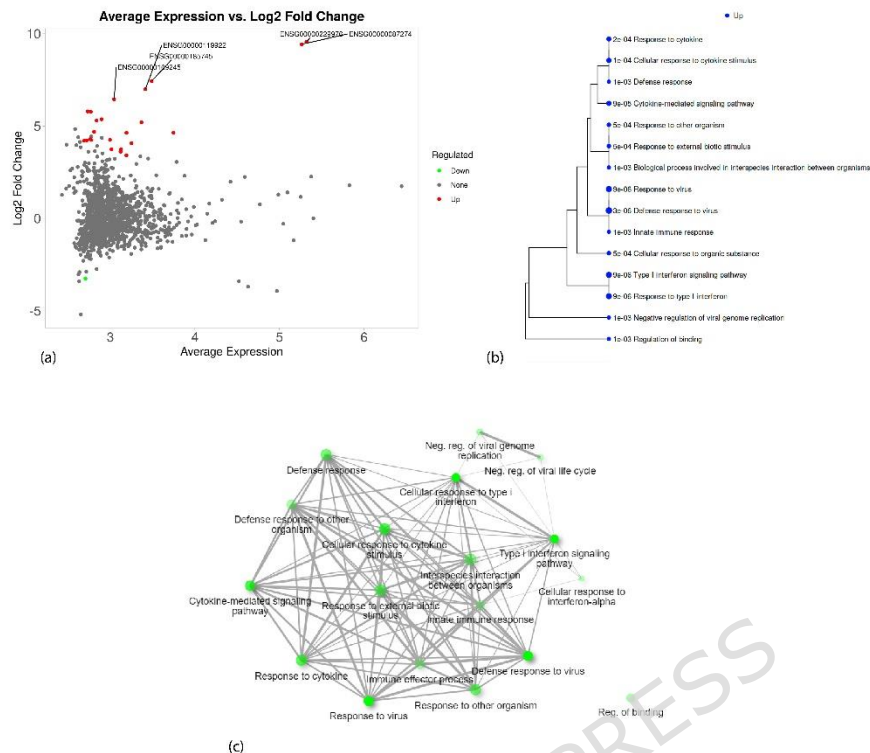


169

170

Fig 3: PCA plot showing the overlapping clusters of host gene expression data

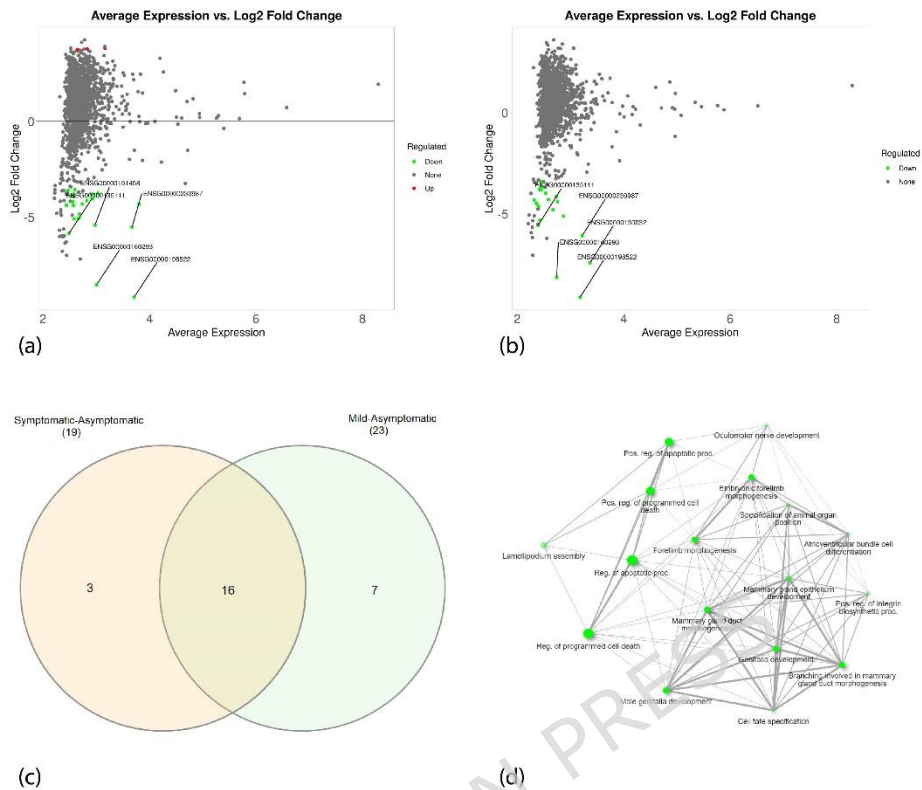
171 Differential expressions of mild and negative patients showed 23 upregulated genes in the mild
 172 group than negative patients. The top five expressed genes, such as, ENSG00000229976
 173 (lncRNA), ENSG00000087274 (*ADD1*), ENSG00000185745 (*IFIT1*), ENSG00000119922
 174 (*IFIT2*), ENSG00000169245 (*CXCL10*) are marked in Fig 4a. After the enrichment analysis of the
 175 upregulated genes, it was evident that mostly virus associated immunological genes were
 176 upregulated in COVID-19 positive patients (Fig 4b). Cellular response to cytokine stimulus, innate
 177 immune response, response to virus, cytokine mediated signaling pathway, Type-1 interferon
 178 signaling pathway etc. were most prominent ones. This analysis followed a protein-protein
 179 interaction network analysis to ensure the association among the pathways (Fig 4c). Immune
 180 response related genes formed a cluster among themselves according to that analysis and binding
 181 regulation gene can be seen distant than the cluster.



182

183 Fig 4: Differential gene expression analysis between Mild and Negative groups. Fig 4(a) shows
 184 MA plot for the differential gene expression of this group. Fig 4(b) showing enrichment analysis
 185 of the upregulated genes and Fig 4(c) showing PPI network among them.

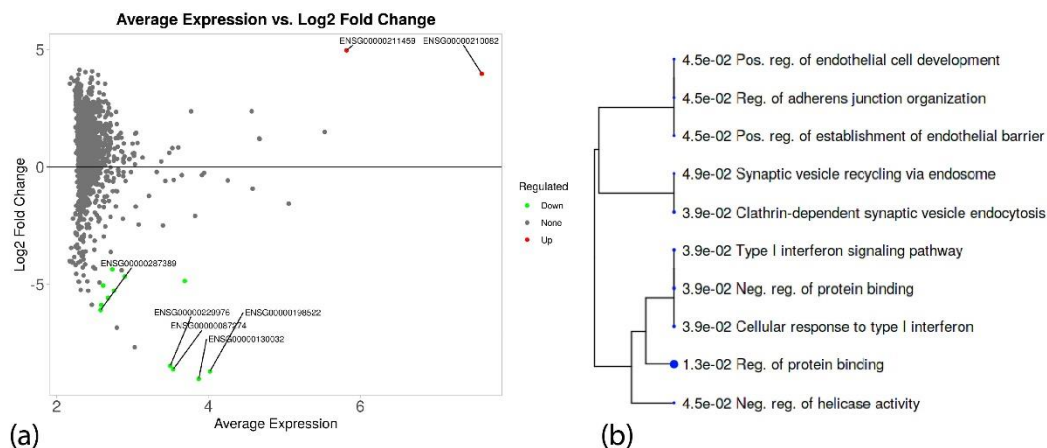
186 Moreover, differential expression analysis of mild vs asymptomatic positive group and
 187 symptomatic (Mild and Severe) vs asymptomatic positive group was performed (Fig 5a, 5b). The
 188 mild and asymptomatic positive group showed 23 downregulated genes and symptomatic vs
 189 asymptomatic group showed 19 downregulated genes. The top expressed genes from both groups
 190 are shown in the MA plot. ENSG00000198522 (*GPNI*), ENSG00000160293 (*VAV2*),
 191 ENSG00000135111 (*TBX3*), ENSG00000151458 (*ANKRD50*), ENSG00000230987. Further
 192 enrichment analysis of the downregulated genes showed 16 common genes, when plotted in Venn
 193 diagram (Fig 5c). These genes showed physiological functional processes in gene ontology
 194 enrichment, and they all fall into one cluster upon network analysis among themselves (Fig 5d).



195

196 Fig 5: MA plot showing differential gene expression in two different groups. Fig 5(a) shows mild
 197 vs asymptomatic group. The top five expressed genes such as, ENSG00000198522 (*GPNI*),
 198 ENSG00000160293 (*VAV2*), ENSG00000135111 (*TBX3*), ENSG00000151458 (*ANKRD50*),
 199 ENSG00000230987 are marked here. Fig 5(b) shows symptomatic vs asymptomatic group. Top
 200 five expressed genes such as, ENSG00000198522 (*GPNI*), ENSG00000160293 (*VAV2*),
 201 ENSG00000130032 (*PRRG3*), ENSG00000230987 and ENSG00000135111 (*TBX3*) are marked
 202 here. Fig 5(c) and Fig 5(d) show the network among the common biological processes.

203 Furthermore, COVID-19 negative group showed 12 downregulated genes than the asymptomatic
 204 group (Fig 6a). The upregulated genes are ENSG00000210082 (*MT-RNR2*), ENSG00000211459
 205 (*MT-RNR1*) and the top expressed downregulated genes are as follows, ENSG00000130032
 206 (*PRRG3*), ENSG00000198522 (*GPNI*), ENSG00000087274 (*ADD1*),
 207 ENSG00000229976 (lncRNA), ENSG00000287389 (lncRNA). The GO biological process
 208 enrichment analysis showed downregulation of immunological signaling genes in negative
 209 patients (Fig 6b).



210

211 Fig 6: (a) MA plot showing differential gene expression between COVID-19 negative and
 212 asymptomatic patients. (b) showing the downregulated genes

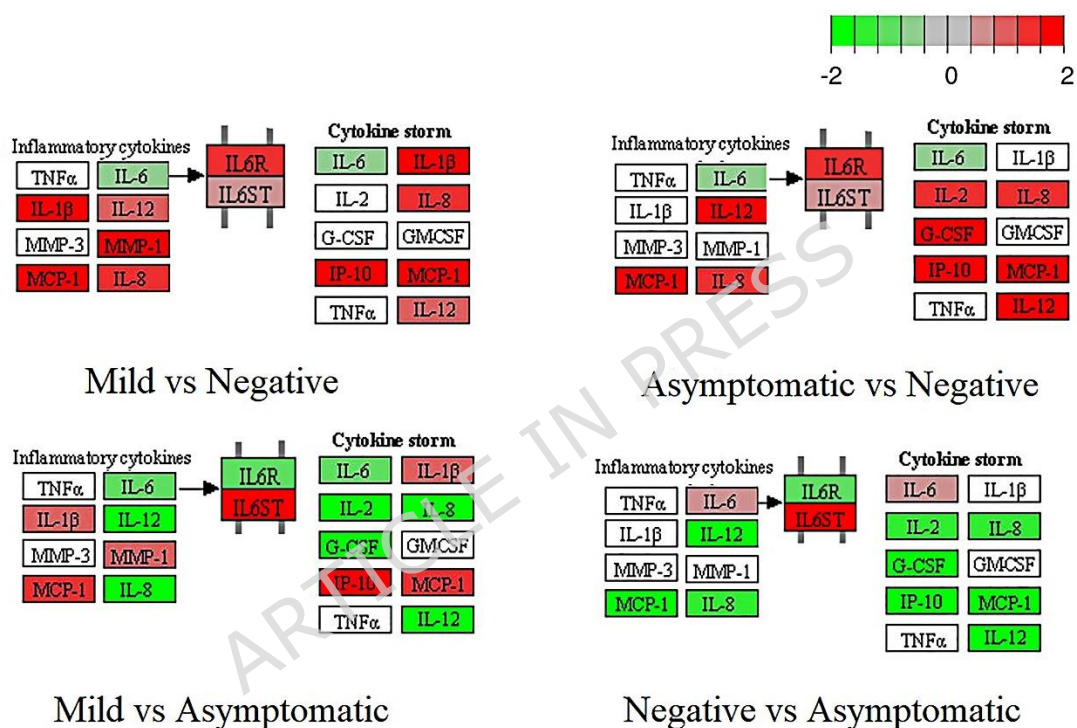
213 Integrative Analysis Reveals Correlation Between Host Genes and 214 Microbial Taxa:

215 The correlation analysis revealed several significant associations that highlight the direct interplay
 216 between host cellular processes and specific microbes (Fig 7; full results in Supplementary File
 217 S5). A significant positive correlation was observed between the abundance of *Pseudomonas sp.*
 218 *LPH1* and the expression of multiple host genes. The strongest of these was with the gene *GPNI*
 219 (Spearman's $\rho = +0.65$, adj. $p = 0.0019$). A significant positive association was also found between
 220 this microbe and *BCL2L14* (Spearman's $\rho = +0.55$, adj. $p = 0.026$).

221 Conversely, the analysis identified a strong and significant negative correlation between the
 222 expression of the host gene *PRRG3* and the abundance of *Moraxella osloensis* (Spearman's $\rho = -$
 223 0.57 , adj. $p = 0.019$). These findings suggest that the presence of specific bacteria, such as
 224 *Pseudomonas* and *Moraxella*, may be directly linked to the modulation of host cellular pathways,
 225 providing a potential mechanistic basis for the different clinical outcomes observed in COVID-19.

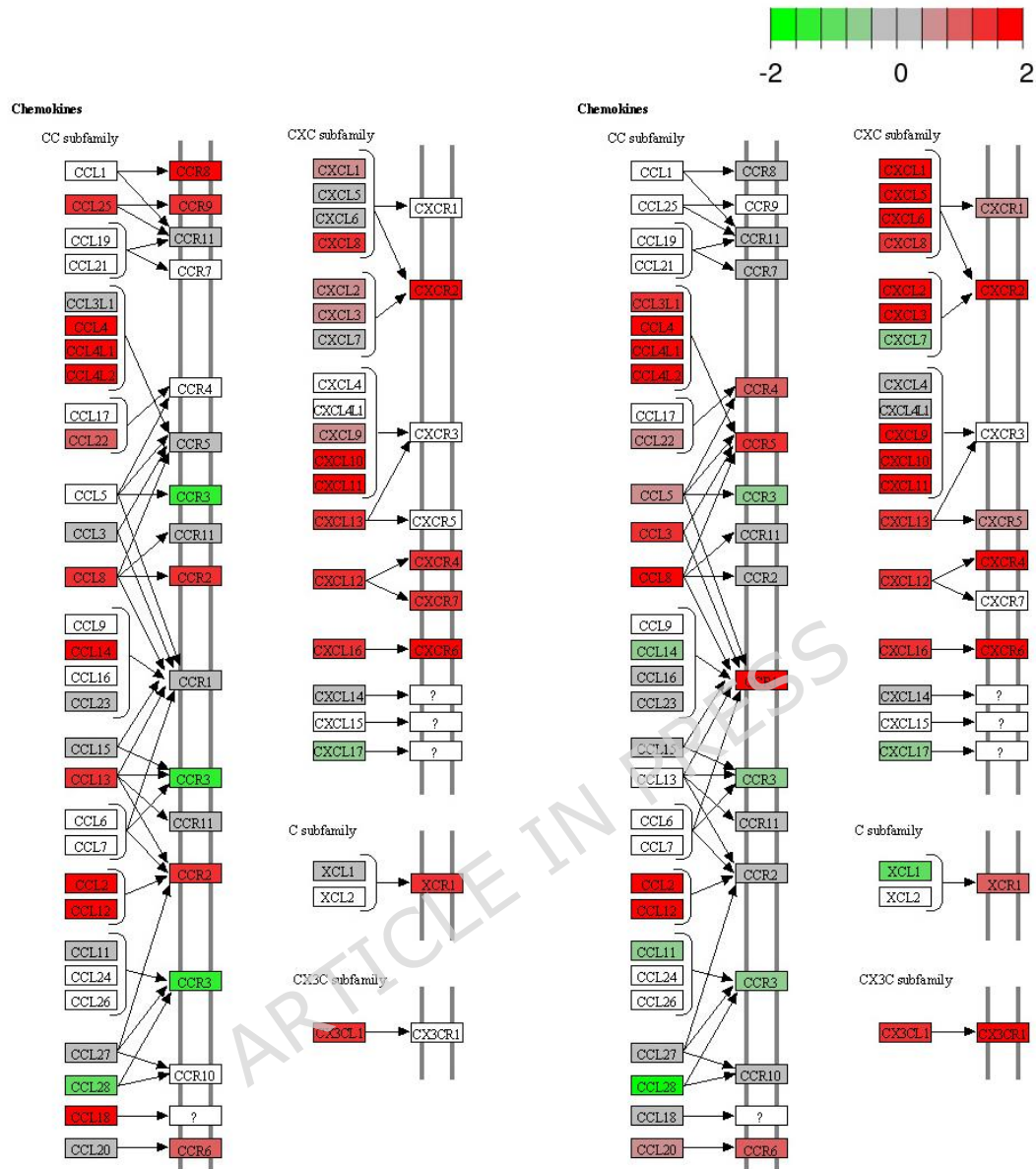
239 were compared with asymptomatic positive samples, inflammatory cytokines were comparatively
 240 downregulated. But the cytokines were upregulated when the order was reversed i.e.,
 241 asymptomatic vs negative.

242 An interesting pattern was found with IL-6 which is the most important cytokine for any viral
 243 infection. In COVID-19 positive cases, IL-6 was found to be moderately downregulated, which is
 244 unusual. But when the cytokine-cytokine receptor signaling was checked, IL-6 receptor was highly
 245 upregulated. Furthermore, MMP-1 was also upregulated in positive cases, which is reported to be
 246 increased with the upregulation of IL-6 [16]. As nasopharyngeal swab was used as the sample,
 247 cytokine level changes were not evident that much. If blood samples were taken, the results would
 248 be more meaningful.



249
 250 Fig 8: Changes in cytokine signaling in different study cohorts. Bright red indicates the most
 251 upregulated and bright green the most downregulated genes. KEGG [17–19] pathway maps were
 252 generated using the Pathview package in R. The panels were assembled using Microsoft Paint for
 253 layout purposes only.

254 Chemokines are an integral part of cytokine storm after a viral infection. Reports suggest
 255 association of CCL2, CCL3, CCL4, CCL7 and CXC subfamily with the severity of cytokine storm.
 256 These chemokines were upregulated in our COVID-19 positive cases as well (Fig 9).
 257 Asymptomatic positive patients showed a slightly different expression pattern of chemokines,
 258 especially the receptors and CXC subfamily, in comparison with COVID-19 negative patients.



259

Mild vs Negative

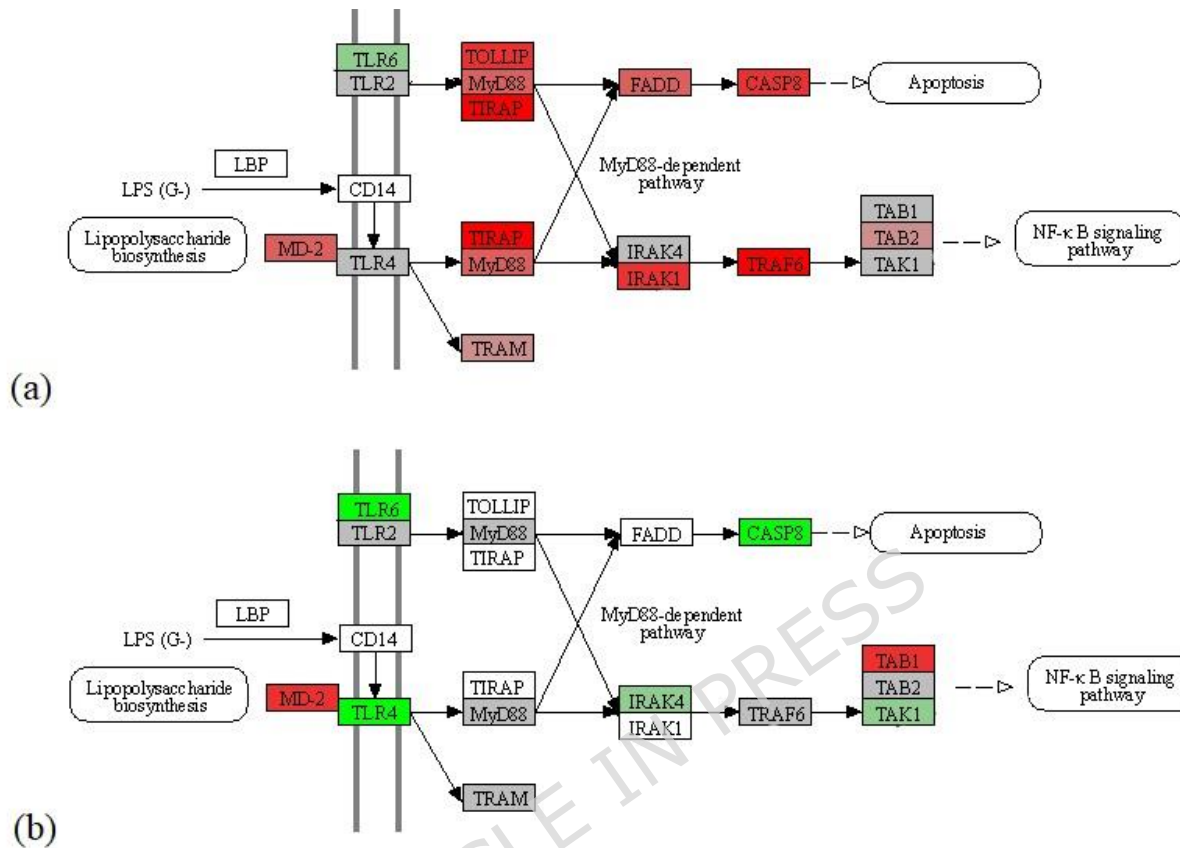
Asymptomatic vs Negative

260 Fig 9: Changes in chemokines and their receptor signaling in different study cohorts. Here bright
 261 red indicates most upregulated, bright green, most downregulated. KEGG [17–19] pathway maps
 262 were generated using the Pathview package in R. The panels were assembled using Microsoft Paint
 263 for layout purposes only

264 TLRs play a major role in the initiation of innate immune responses, with the production of
 265 inflammatory cytokines, type-1 IFN and other mediators. TLR4 stimulation induced the strongest
 266 effect in terms of cytokine release (Fig 10a).

267 Here in this study, asymptomatic positive patients showed downregulation of TLR4 in comparison
 268 with negative samples (Fig 10b). As TLR4 plays a major role in the initiation of cytokine storm,

269 it may be suggested from this data that, downregulation of TLR4 could contribute to the observed
 270 asymptomatic clinical outcome.



271

272 Fig 10: Partial demonstration of Toll like receptor signaling pathway in different groups. (a) Mild
 273 vs Negative and, (b) Asymptomatic Positive vs Negative. KEGG [17–19] pathway maps were
 274 generated using the Pathview package in R. The panels were assembled using Microsoft Paint for
 275 layout purposes only.

276

277 Discussion:

278 The interconnection between human microbiome and disease development has already been
 279 studied well by the scientific community [20–22]. Microbiome composition is shaped by various
 280 environmental factors, and in turn, influences host health and immune function. During the
 281 COVID-19 pandemic, one of the major questions arose regarding the underlying factors
 282 contributing to variable disease severity. While most of the research proved the association of
 283 comorbidity, age, sex, and immunosuppression [23–25], the potential influence of the human
 284 microbiome has also garnered attention. In particular, the microbiome's role in explaining the high
 285 prevalence of asymptomatic infections, often critical in silent transmission chains, remains an area
 286 of active investigation.

287 In this study, nasopharyngeal samples of different severity groups of COVID-19 patients were
 288 subjected to metatranscriptomic analysis for a better understanding of taxonomic and functional

289 profile. Unbiased metatranscriptomic data helps to effectively characterize the microbiome and
290 host response in COVID-19.

291 Alpha diversity measured using Shannon and Simpson Diversity metrics showed significant
292 species diversity within the sample groups in terms of prokaryotes. But widespread distribution
293 was observed in terms of Eukaryotes (Fig 1d), suggesting greater heterogeneity among these
294 individuals, potentially reflecting increased opportunistic fungal colonization, which has been
295 commonly reported in severe COVID-19 cases [11]. However, between diversity analysis of
296 different groups created a separate cluster for Asymptomatic group for both the prokaryotes and
297 eukaryotes, highlighting the unique species diversity in the group. The rest of the groups showed
298 a closer clustering, suggesting a more stable eukaryotic community.

299 The tendency to acquire more pathogenic bacteria increases with severity. From the Relative
300 Abundance (RA) analysis, it's evident that pathogenic strains like *Acinetobacter* and *Pseudomonas*
301 were significantly high in severe cases. Evidence showed the fungal association with the COVID-
302 19 disease, which can sometimes affect the mortality or immune response in the host body [27,28].
303 In some cases, people also get fungal infection after recovering from viral diseases [29].

304 According to González. R et al., microbiomes have a significant and broad influence in shaping
305 their host biology, specifically in the immunity and host defense responses [30]. It directly impacts
306 the outcomes of infections by pathogens. This is also reflected in the microbiome
307 metatranscriptomic analysis of different severity in this study. The asymptomatic group of patients
308 did not show any immune response related gene expression rather than showing regular cellular
309 function related genes. This implies a minimum amount of viral interference and an active
310 microbial response. Moreover, the severe and mild group showed a substantial rise of immune
311 response. The data revealed significant mechanisms pertaining to the inhibition of host type I
312 interferon signaling and the stimulation of host autophagy, which are indicative of both viral
313 reproduction in motion and a more regulated immune response. Additionally, there was evidence
314 of elevated cellular stress responses and widespread viral subversion of host cellular pathways and
315 molecular processes. Moreover, the detection of β -lactamase activity in the GO term enrichment
316 analysis indicates not only the presence but also the functional expression of ARGs. This is further
317 supported by the circos plot, where high-intensity signals, particularly from TEM1-D, confirm its
318 prevalence across all severity groups, while unique ARG signatures were statistically enriched in
319 the asymptomatic cohort. Such resistome variation may influence host-microbiome interactions,
320 potentially modulating immune responses and contributing to reduced symptom manifestation
321 [31–33].

322 However, different research works have shown how the respiratory microbiome is changing with
323 the COVID-19 disease [34,35]. In this study, COVID-19 related differential host gene expression
324 revealed distinct transcriptional signatures across the study cohorts. COVID-19 positive patients
325 had twenty-three upregulated genes than the negative patients. The upregulated genes were related
326 to responses to viral infection as cytokine storm is already reported to be associated with SARS-
327 CoV-2 infection [36,37]. Further analysis demonstrated the highly interconnected protein-protein
328 interaction network among the upregulated genes.

329 Additionally, sixteen frequently downregulated genes were identified based on the differentially
330 expressed genes shown in the Venn diagram (Fig 5c) in order to determine the genetic signatures
331 unique to asymptomatic positive patients. These genes were mainly linked to physiological

332 processes, especially those related to reproduction and development, which might be a reflection
333 of underlying pre-existing health conditions in these people.

334 In addition, differential expression analysis of COVID-19 negative and asymptomatic positive
335 group showed downregulation of immunological signaling genes in negative patients (Fig 6). As
336 they were not affected with the SARS-CoV-2 virus infection, their viral responses were
337 comparatively lower than the other.

338 The findings of this study are further strengthened by the integrated correlation analysis, which
339 moves beyond descriptive comparisons to establish direct statistical links between host and
340 microbial activities. For instance, the strong positive correlation between *Pseudomonas sp.* and
341 host genes like *GPN1* and *BCL2L14* is particularly noteworthy. As *Pseudomonas* is a known
342 opportunistic pathogen, its association with genes involved in fundamental cellular processes
343 (GTPase activity and apoptosis regulation [38]) suggests a potential mechanism by which this
344 microbe could influence host cell function during infection.

345 Similarly, the negative correlation between *Moraxella osloensis* and the host gene *PRRG3*
346 provides a specific, testable hypothesis for future research [39]. *PRRG3* encodes a single-pass
347 transmembrane protein containing a γ -carboxyglutamic acid (Gla) domain, consistent with a role
348 in membrane-associated signaling or regulation [40].
349 The observed inverse correlation therefore represents a clear, testable link between the local
350 microbiota and host cellular regulatory function, in line with growing evidence that microbial
351 communities can modulate host gene expression and signaling pathways [41].

352 KEGG pathway analysis is widely used for understanding the biological relevance of the disease
353 or infection with the host body [19]. Different studies have demonstrated the molecular landscape
354 and biomarkers associated with SARS-CoV-2 viral infections using this method [42,43] but in this
355 study a number of immunological signaling was focused on understanding the host response to the
356 infection. Upon entry into the host and subsequent dissemination into the bloodstream, SARS-
357 CoV-2 triggers the activation of immune cells, leading to the release of various pro-inflammatory
358 cytokines. This, in turn, facilitates the release of inflammatory cytokines; in some cases, an
359 exaggerated immune response leads to a cytokine storm, contributing to disease severity and multi-
360 organ dysfunction [44]. In agreement with the available reports on “cytokine storm”, this study
361 also found out the upregulation of some pro-inflammatory cytokines IL-1 β and IL-12, which in
362 turn upregulated cytokine storm of IL-8, IL-12, MCP-1, IP-10. In addition, asymptomatic positive
363 samples showed upregulated cytokines against COVID-19 negative samples. The reason here lies
364 in the threshold level of the expression [45]. As the negative samples are not affected by SARS-
365 CoV-2, they are not expected to exhibit a cytokine storm. Though the asymptomatic positive cases
366 may not show symptoms, they are affected by the virus. Thus, they have slight cytokine
367 upregulation. However, this upregulation remains below the threshold needed to trigger symptoms,
368 possibly due to internal regulatory mechanisms. Same goes for the cytokines in asymptomatic
369 positive cases. Chemokines are reported to be involved in COVID-19 progression and severity
370 [46] which was also seen in this study. *CCL2*, *CCL3*, *CCL4*, *CCL7* and *CXC* subfamily were
371 upregulated in the COVID-19 positive cases.

372 Toll-like receptors (TLRs) are vital components of the innate immune system, functioning as
373 pattern recognition receptors that detect conserved microbial structures and initiate host defense
374 mechanisms [47]. To date, 13 mammalian TLRs (TLR1–TLR13) have been identified, each
375 exhibiting distinct ligand specificities and pattern recognition capabilities [48]. Though TLR4

376 expression is majorly dependent on lipopolysaccharide (LPS), some studies reported that it is
377 correlated with viral disease severity [49]. This expression mediates the infection symptoms as
378 well. Here, TLR4 has lower expression in asymptomatic positive cases than healthy individuals
379 raising the possibility that this differential expression may contribute to the lack of symptom
380 development in these patients. However since our study utilized bulk metatranscriptomic data from
381 nasopharyngeal swabs, which contain a heterogeneous mixture of cell types, including epithelial
382 cells and various immune cells [50] and TLR4 is known to be highly expressed in innate immune
383 cells [48], it is possible that the observed downregulation in the asymptomatic cohort reflects a
384 different cellular composition in the collected swabs (e.g., a lower proportion of immune cells)
385 rather than a true biological downregulation within a specific cell type. We acknowledge this as a
386 limitation of our study. Future research using single-cell sequencing would be necessary to
387 deconvolve this effect and confirm the cell-specific expression of TLR4 [50].

388 In conclusion, this study reveals distinct microbiome and host transcriptomic profiles across
389 COVID-19 severity groups, with asymptomatic cases showing unique microbial diversity, reduced
390 immune activation, and lower TLR4 expression. Downregulation of pro-inflammatory cytokines
391 and interleukins in this group suggests intrinsic immune regulation may limit symptom
392 development. The detection of active antimicrobial resistance genes further underscores the need
393 for monitoring secondary pathogens in COVID-19. These findings highlight the value of
394 integrating microbiome and host transcriptome analyses to better understand variable disease
395 outcomes, warranting validation in larger, diverse cohorts.

396 **Methodology:**

397 **Ethics Statement:** This study was conducted in accordance with the ethical principles
398 outlined in the Declaration of Helsinki. The methodology and protocol used for this study were
399 reviewed and approved by the Human Research Ethics Review Committee, National Institute of
400 Laboratory Medicine & Referral Center (NILMRC), Dhaka, Bangladesh. Informed verbal consent
401 was obtained from all participants prior to sample collection, as approved by the IRB, given
402 pandemic-related restrictions on physical contact.

403 **Sampling and Transcriptome Sequencing:** Nasopharyngeal samples from forty
404 different people were collected for the study. COVID-19 positive and suspected individuals of
405 different categories were included in the study after RT-PCR test. We note that patient severity
406 classification was based on clinical symptoms and Ct values; chest X-rays or other clinical imaging
407 were not available for assessing lung condition.

408 The cohort had individuals from ICU, COVID-19 positive, negative, reinfected, recovered, and
409 asymptomatic positive patients as well. Asymptomatic positive patients were healthcare staff who
410 had to go through routine checkup of COVID-19 RT-PCR test. However, the patients were
411 enrolled and categorized into four cohorts based on clinical presentation, SARS-CoV-2 RT-PCR
412 status, and duration of symptoms as described in Table 1. Detailed metadata is available in S1.

413
414
415
416

417 Table 1: Description of the study cohort. Here n represents the sample number

Cohort Name	Description of the Cohort
Negative Cohort (n=12)	The individuals who were negative for SARS-CoV-2 by RT-PCR and were free of symptoms of COVID-19-like illness (i.e., fever, cough, shortness of breath, loss of smell or taste) for at least two weeks.
Asymptomatic Cohort (n=7)	Asymptomatic SARS-CoV-2 positive individuals were identified through routine surveillance screening of healthcare staff. These individuals had a positive RT-PCR confirmed but were totally free of any COVID-19-like symptoms for the entire two-week period following their positive test.
Mild Cohort (n=11)	This cohort included hospitalized, RT-PCR-confirmed SARS-CoV-2 positive patients with mild to moderate symptoms of the disease. None of the patients in this cohort developed severe complications (i.e., requiring high-flow oxygen, non-invasive or invasive mechanical ventilation) over a two-week observation period following diagnosis.
Severe Cohort (n=10)	Hospitalized, RT-PCR-confirmed SARS-CoV-2 positive patients who developed severe disease requiring Intensive Care Unit (ICU) admission. Development of critical illness typically occurred between 5 to 7 days of initial symptom onset or diagnosis.

418
419 The samples were collected using universal transfer media (UTM) and transported to the
420 laboratory under a maintained cold chain. Upon arrival, samples were immediately stored in -80°C
421 before RNA extraction. Proper safety measures were taken to avoid RNase contamination during
422 handling the sample. RNA was extracted using the ReliaPrep™ Viral TNA Miniprep System,
423 Promega (USA). The RNA samples were further stored in -80°C before sequencing was
424 performed. The RNA concentrations were measured using NanoDrop™ One (Thermo Scientific
425 Inc. USA). Sequencing was performed at the Genomic Research Laboratory, BCSIR Dhaka
426 Laboratory, BCSIR, Dhaka, Bangladesh. Illumina NextSeq550 platform was used for sequencing
427 purposes, and the sequencing library was prepared using TruSeq RNA Library Preparation Kit as
428 per the manufacturers protocol. The protocol involved rRNA removal step using Ribo-zero rRNA
429 removal beads. Ribosomal RNA depletion efficiency was assessed computationally by quantifying
430 reads overlapping annotated rRNA loci using BED-based genome interval intersection (bedtools).
431 The final library concentration was quantified using a Quantus fluorometer (Promega, USA) prior
432 to sequencing. We note that RNA integrity (e.g., RIN) was not formally assessed due to the
433 unavailability of specialized electrophoretic equipment, and we also acknowledge that
434 nasopharyngeal swabs frequently yield RNA of variable and often reduced integrity. However,
435 RNA integrity and positional coverage bias were assessed computationally using RSeQC (v5.0.4)
436 [51]. Read distribution across genomic features (CDS exons, 5'UTR, 3'UTR, and introns) was
437 calculated using the read_distribution.py module with the GRCh38 reference annotation. This
438 analysis was used to evaluate potential 5'–3' degradation bias and overall transcript coverage
439 uniformity.

440 Preprocessing and alignment were performed using RNA Seq Alignment app software. Quality
441 control and adapter trimming were performed using FastQC and Trimmomatic within the pipeline,

442 and high-quality reads were aligned to the human reference genome (Ensembl GRCh38) using the
443 STAR aligner [52]. Mapped reads corresponding to human transcripts were retained for host
444 differential expression analysis. Unmapped reads were extracted and used for microbial taxonomic
445 and functional analysis. This host read removal step ensured that microbial reads were not
446 confounded by human sequences and reduced the likelihood of cross-alignment errors between
447 host and microbial genomes. A list of software packages and their versions is available in the
448 supplementary file S4.

449
450 **Microbiome diversity and antibiotic resistance analysis:** Taxonomic
451 classification of the microbial reads was performed using the CZID pipeline. This pipeline
452 determines the abundance of bacteria, archaea, viruses, and eukaryotes by aligning sequenced
453 reads against the NCBI RefSeq database. Different microbial population (Prokaryotes and
454 Eukaryotes) present in the nasopharyngeal samples were checked using different R packages
455 (version 4.2), to determine the association of COVID-19 severity with microbial diversity.
456 "Phyloseq" [53] and "Vegan" [54] were used to conduct normalization procedures via rarefaction
457 and to assess disparities in abundances. These packages facilitated the comprehensive analysis of
458 diversity and composition across various sample groups. Alpha diversity (differences within the
459 sample groups) metrics were assessed employing the Wilcoxon Rank Signed test, while
460 PERMANOVA, utilizing the Adonis test with 999 permutations (implemented through the
461 Set.seed function), was employed to evaluate discrepancies in beta diversity. Furthermore, for the
462 graphical representation of diversity measures and compositional analysis, R packages such as
463 "ggpubr" and "ggplot2" were employed [55]. Antibiotic resistant genes of the data were checked
464 using CZID [56] platform, which utilizes the CARD database for resistance gene identification
465 and classification. A Circos plot was generated using "circlize" R package [57] based on the
466 number of hits on each resistant gene.

467 Sterile handling procedures were maintained throughout sample processing to reduce the risk of
468 reagent or environmental contamination. Accordingly, interpretations of potentially pathogenic
469 bacterial taxa and ARGs were made with caution, acknowledging the potential influence of low-
470 level contaminant signals.

471 To identify differentially abundant ARGs in the asymptomatic group, raw ARG counts were
472 analyzed using the DESeq2 package (v1.48.2) in R (v4.3.3). The analysis was performed by
473 comparing the asymptomatic cohort against a combined symptomatic cohort (mild and severe).
474 Genes with an FDR-adjusted p-value (padj) less than 0.05 were considered statistically significant.

475
476 **Microbial metatranscriptomics, host differential gene expression and**
477 **enrichment analysis:** Microbial metatranscriptomics analysis was performed using
478 Microbiome Metatranscriptomics pipeline (version 10.2) from BaseSpace, Illumina. This pipeline
479 performs functional profiling by aligning reads against the UniRef (UniProt Reference Clusters)
480 database for bacteria, archaea, viruses, and eukaryotes. The resulting raw data was plotted in
481 heatmap using Pheatmap package in R. Differential gene expression of the host genome is
482 important to determine the functional changes of human body due to diverse microbial community.
483 DESeq2 package [58] was used for differential gene expression analysis and several other

484 bioinformatic tools were used for gene enrichment analysis and protein-protein interaction
485 prediction. We used raw gene counts as the direct input for DESeq2, as recommended by the tool's
486 authors. This method is preferred over methods using normalized counts (like TPM or RPKM)
487 because DESeq2's statistical model inherently accounts for library size and, by performing
488 comparisons on a per-gene basis, is not confounded by gene length differences.

489 **Integrated Host-Microbiome Correlation Analysis:** To investigate the direct
490 relationship between the host transcriptome and the microbiome, an integrated correlation analysis
491 was performed. First, all 11 significant differentially expressed genes (DEGs) ($FDR < 0.05$,
492 $|\log_2FC| > 1$) were identified from the host transcriptome data comparing symptomatic (Mild and
493 Severe) and asymptomatic cohorts. Separately, the top 30 most abundant microbial taxa were
494 identified based on their mean relative abundance across the samples.

495 Spearman's rank correlation was then calculated for each pair of selected host genes and microbial
496 taxa using the `corr.test` function from the 'psych' package in R (v4.2.0). P-values were adjusted for
497 multiple comparisons using the False Discovery Rate (FDR) method. Correlations with an FDR-
498 adjusted p-value < 0.05 were considered statistically significant. The results were visualized using
499 the 'pheatmap' package.

500

501 **Signaling pathway analysis:** A software package Pathview [59] was used for pathway-
502 based data integration and visualization. Pathview generates native KEGG pathway graphs [17],
503 hence is natural and more readable for humans. Here different colors indicate the most upregulated
504 and downregulated genes. Important immunological pathways were analyzed and compared
505 among different study groups for finding associations using different statistical analysis.

506 Declaration

507 Ethical approval and consent to participate

508 The ethical permission of the protocol for sample collection from patients, sample processing, and
509 other consecutive laboratory work was taken from the National Institute of Laboratory Medicine
510 and Referral Center (NILMRC) of Bangladesh.

511 Availability of data and material

512 All the data related to this manuscript is available in the supplement files and all the raw data is
513 uploaded to NCBI under the accession number of PRJNA1298058. Formal permission was taken
514 from Kanehisa laboratories to publish the result of using KEGG software, both in print and digital,
515 under the CC BY 4.0 open access license.

516 Competing interests

517 The authors declare that they have no competing interests

518 Funding

519 This work has been funded by the Ministry of Science and Technology, Bangladesh.

520 **Authors' contributions**

521 **Experimental Design:** Murshed Hasan Sarkar, Sanjana Fatema Chowdhury, Salim Khan

522 **Sample Collection:** Md. Maruf Ahmed Molla, Tasnim Nafisa, Mahmuda Yeasmin, Asish Kumar
523 Ghosh

524 **Library Preparation and Sequencing:** Murshed Hasan Sarkar, Md. Saddam Hossain, Iffat Jahan

525 **Data Analysis and Primary Analysis:** Sanjana Fatema Chowdhury, Murshed Hasan Sarkar, Syed
526 Muktadir Al Sium, Tanay Chakrovarty

527 **Manuscript Preparation:** Sanjana Fatema Chowdhury, Murshed Hasan Sarkar, Syed Muktadir
528 Al Sium, Showti Raheel Naser

529 **Logistic Support:** Md. Ahashan Habib, Shahina Akter, Tanjina Akhtar Banu, Barna Goswami

530 **Acknowledgements**

531 The authors would like to acknowledge National Institute of Laboratory Medicine & Referral
532 Center (NILMRC), Dhaka, Bangladesh for the support during sample collection. The authors also
533 acknowledge Bangladesh Council of Scientific and Industrial Research (BCSIR), Bangladesh and
534 Ministry of Science and Technology, Bangladesh for the funding and infrastructure support.

535 **References:**

536 1. Zhu N, Zhang D, Wang W, Li X, Yang B, Song J, et al. A Novel Coronavirus from Patients with
537 Pneumonia in China, 2019. *N Engl J Med.* 2020;382: 727–733. doi:10.1056/nejmoa2001017

538 2. Salata C, Calistri A, Parolin C, Palù G. Coronaviruses: a paradigm of new emerging zoonotic
539 diseases. *Pathog Dis.* 2019;77. doi:10.1093/femspd/ftaa006

540 3. Tan W, Zhao X, Ma X, Wang W, Niu P, Xu W, et al. A Novel Coronavirus Genome Identified in a
541 Cluster of Pneumonia Cases - Wuhan, China 2019-2020. *China CDC Wkly.* 2020;2: 61–62.

542 4. Du Toit A. Outbreak of a novel coronavirus. *Nat Rev Microbiol.* 2020;18: 123.
543 doi:10.1038/s41579-020-0332-0

544 5. Zhou F, Yu T, Du R, Fan G, Liu Y, Liu Z, et al. Clinical course and risk factors for mortality of adult
545 inpatients with COVID-19 in Wuhan, China: a retrospective cohort study. *Lancet Lond Engl.* 2020;395:
546 1054–1062. doi:10.1016/S0140-6736(20)30566-3

547 6. Kumar A, Narayan RK, Prasoon P, Kumari C, Kaur G, Kumar S, et al. COVID-19 Mechanisms in the
548 Human Body—What We Know So Far. *Front Immunol.* 2021;12. doi:10.3389/fimmu.2021.693938

549 7. Daamen AR, Bachali P, Owen KA, Kingsmore KM, Hubbard EL, Labonte AC, et al. Comprehensive
550 transcriptomic analysis of COVID-19 blood, lung, and airway. *Sci Rep.* 2021;11. doi:10.1038/s41598-021-
551 86002-x

- 552 8. Xiong Y, Liu Y, Cao L, Wang D, Guo M, Jiang A, et al. Transcriptomic characteristics of
553 bronchoalveolar lavage fluid and peripheral blood mononuclear cells in COVID-19 patients. *Emerg*
554 *Microbes Infect.* 2020;9: 761–770. doi:10.1080/22221751.2020.1747363
- 555 9. Hoque MN, Rahman MS, Ahmed R, Hossain MS, Islam MS, Islam T, et al. Diversity and genomic
556 determinants of the microbiomes associated with COVID-19 and non-COVID respiratory diseases. *Gene*
557 *Rep.* 2021;23: 101200. doi:10.1016/j.genrep.2021.101200
- 558 10. Chen N, Zhou M, Dong X, Qu J, Gong F, Han Y, et al. Epidemiological and clinical characteristics
559 of 99 cases of 2019 novel coronavirus pneumonia in Wuhan, China: a descriptive study. *Lancet Lond*
560 *Engl.* 2020;395: 507–513. doi:10.1016/S0140-6736(20)30211-7
- 561 11. Hoque MN, Sarkar MMH, Rahman MS, Akter S, Banu TA, Goswami B, et al. SARS-CoV-2 infection
562 reduces human nasopharyngeal commensal microbiome with inclusion of pathobionts. *Sci Rep.* 2021;11:
563 24042. doi:10.1038/s41598-021-03245-4
- 564 12. Avraham R, Haseley N, Fan A, Bloom-Ackermann Z, Livny J, Hung DT. A highly multiplexed and
565 sensitive RNA-seq protocol for simultaneous analysis of host and pathogen transcriptomes. *Nat Protoc.*
566 2016;11: 1477–1491. doi:10.1038/nprot.2016.090
- 567 13. Zhang H, Ai J-W, Yang W, Zhou X, He F, Xie S, et al. Metatranscriptomic Characterization of
568 Coronavirus Disease 2019 Identified a Host Transcriptional Classifier Associated With Immune Signaling.
569 *Clin Infect Dis.* 2021;73: 376–385. doi:10.1093/cid/ciaa663
- 570 14. Haiminen N, Utro F, Seabolt E, Parida L. Functional profiling of COVID-19 respiratory tract
571 microbiomes. *Sci Rep.* 2021;11. doi:10.1038/s41598-021-85750-0
- 572 15. Tang F, Barbacioru C, Wang Y, Nordman E, Lee C, Xu N, et al. mRNA-Seq whole-transcriptome
573 analysis of a single cell. *Nat Methods.* 2009;6: 377–382. doi:10.1038/nmeth.1315
- 574 16. Li Y, Samuvel DJ, Sundararaj KP, Lopes-Virella MF, Huang Y. IL-6 and high glucose synergistically
575 upregulate MMP-1 expression by U937 mononuclear phagocytes via ERK1/2 and JNK pathways and c-
576 Jun. *J Cell Biochem.* 2010;110: 248–259. doi:10.1002/jcb.22532
- 577 17. Kanehisa M, Furumichi M, Sato Y, Matsuura Y, Ishiguro-Watanabe M. KEGG: biological systems
578 database as a model of the real world. *Nucleic Acids Res.* 2025;53: D672–D677.
579 doi:10.1093/nar/gkae909
- 580 18. Kanehisa M. Toward understanding the origin and evolution of cellular organisms. *Protein Sci*
581 *Publ Protein Soc.* 2019;28: 1947–1951. doi:10.1002/pro.3715
- 582 19. Kanehisa M, Goto S. KEGG: kyoto encyclopedia of genes and genomes. *Nucleic Acids Res.*
583 2000;28: 27–30. doi:10.1093/nar/28.1.27
- 584 20. Waldman AJ, Balskus EP. The Human Microbiota, Infectious Disease, and Global Health:
585 Challenges and Opportunities. *ACS Infect Dis.* 2018;4: 14–26. doi:10.1021/acsinfectdis.7b00232
- 586 21. Wang B, Yao M, Lv L, Ling Z, Li L. The Human Microbiota in Health and Disease. *Engineering.*
587 2017;3: 71–82. doi:10.1016/j.eng.2017.01.008

- 588 22. Karkman A, Lehtimäki J, Ruokolainen L. The ecology of human microbiota: dynamics and
589 diversity in health and disease. *Ann N Y Acad Sci.* 2017;1399: 78–92. doi:10.1111/nyas.13326
- 590 23. Cho SI, Yoon S, Lee H-J. Impact of comorbidity burden on mortality in patients with COVID-19
591 using the Korean health insurance database. *Sci Rep.* 2021;11. doi:10.1038/s41598-021-85813-2
- 592 24. Osibogun A, Balogun M, Abayomi A, Idris J, Kuyinu Y, Odukoya O, et al. Outcomes of COVID-19
593 patients with comorbidities in southwest Nigeria. Olusanya BO, editor. *PLOS ONE.* 2021;16: e0248281.
594 doi:10.1371/journal.pone.0248281
- 595 25. Yin T, Li Y, Ying Y, Luo Z. Prevalence of comorbidity in Chinese patients with COVID-19:
596 systematic review and meta-analysis of risk factors. *BMC Infect Dis.* 2021;21. doi:10.1186/s12879-021-
597 05915-0
- 598 26. Lopez SMC, Martin JM, Johnson M, Kurs-Lasky M, Horne WT, Marshall CW, et al. A method of
599 processing nasopharyngeal swabs to enable multiple testing. *Pediatr Res.* 2019;86: 651–654.
600 doi:10.1038/s41390-019-0498-1
- 601 27. Peng J, Wang Q, Mei H, Zheng H, Liang G, She X, et al. Fungal co-infection in COVID-19 patients:
602 evidence from a systematic review and meta-analysis. *Aging.* 2021;13: 7745–7757.
603 doi:10.18632/aging.202742
- 604 28. Verweij PE, Gangneux J-P, Bassetti M, Brüggemann RJM, Cornely OA, Koehler P, et al. Diagnosing
605 COVID-19-associated pulmonary aspergillosis. *Lancet Microbe.* 2020;1: e53–e55. doi:10.1016/S2666-
606 5247(20)30027-6
- 607 29. Canning B, Senanayake V, Burns D, Moran E, Dedicoat M. Post-influenza aspergillus ventriculitis.
608 *Clin Infect Pract.* 2020;7–8: 100026. doi:10.1016/j.clinpr.2020.100026
- 609 30. González R, Elena SF. The Interplay between the Host Microbiome and Pathogenic Viral
610 Infections. Prasad VR, editor. *mBio.* 2021;12. doi:10.1128/mbio.02496-21
- 611 31. Palleja A, Mikkelsen KH, Forslund SK, Kashani A, Allin KH, Nielsen T, et al. Recovery of gut
612 microbiota of healthy adults following antibiotic exposure. *Nat Microbiol.* 2018;3: 1255–1265.
613 doi:10.1038/s41564-018-0257-9
- 614 32. Zuo T, Zhang F, Lui GCY, Yeoh YK, Li AYL, Zhan H, et al. Alterations in Gut Microbiota of Patients
615 With COVID-19 During Time of Hospitalization. *Gastroenterology.* 2020;159: 944-955.e8.
616 doi:10.1053/j.gastro.2020.05.048
- 617 33. Umeda L, Torres A, Kunihiro BP, Rubas NC, Wells RK, Phankitnirundorn K, et al. Immuno-
618 Microbial Signature of Vaccine-Induced Immunity against SARS-CoV-2. *Vaccines.* 2024;12: 637.
619 doi:10.3390/vaccines12060637
- 620 34. Ng DL, Granados AC, Santos YA, Servellita V, Goldgof GM, Meydan C, et al. A diagnostic host
621 response biosignature for COVID-19 from RNA profiling of nasal swabs and blood. *Sci Adv.* 2021;7:
622 eabe5984. doi:10.1126/sciadv.abe5984
- 623 35. Hyblova M, Hadzega D, Babisova K, Krumpolec P, Gnip A, Sabaka P, et al. Metatranscriptome
624 Analysis of Nasopharyngeal Swabs across the Varying Severity of COVID-19 Disease Demonstrated

- 625 Unprecedented Species Diversity. *Microorganisms*. 2023;11: 1804.
626 doi:10.3390/microorganisms11071804
- 627 36. Huang C, Wang Y, Li X, Ren L, Zhao J, Hu Y, et al. Clinical features of patients infected with 2019
628 novel coronavirus in Wuhan, China. *The Lancet*. 2020;395: 497–506. doi:10.1016/s0140-6736(20)30183-
629 5
- 630 37. Liu Y, Zhang C, Huang F, Yang Y, Wang F, Yuan J, et al. Elevated plasma levels of selective
631 cytokines in COVID-19 patients reflect viral load and lung injury. *Natl Sci Rev*. 2020;7: 1003–1011.
632 doi:10.1093/nsr/nwaa037
- 633 38. Nuñez G, Clarke MF. The Bcl-2 family of proteins: regulators of cell death and survival. *Trends*
634 *Cell Biol*. 1994;4: 399–403. doi:10.1016/0962-8924(94)90053-1
- 635 39. Lin Z, Jiang Y, Liu H, Yang J, Yang B, Zhang K, et al. Airway microbiota and immunity associated
636 with chronic obstructive pulmonary disease severity. *J Transl Med*. 2025;23: 962. doi:10.1186/s12967-
637 025-06986-2
- 638 40. Zhang E, He J, Zhang H, Shan L, Wu H, Zhang M, et al. Immune-Related Gene-Based Novel
639 Subtypes to Establish a Model Predicting the Risk of Prostate Cancer. *Front Genet*. 2020;11: 595657.
640 doi:10.3389/fgene.2020.595657
- 641 41. Daniel N, Lécuyer E, Chassaing B. Host/microbiota interactions in health and diseases—Time for
642 mucosal microbiology! *Mucosal Immunol*. 2021;14: 1006–1016. doi:10.1038/s41385-021-00383-w
- 643 42. Tian W, Zhang N, Jin R, Feng Y, Wang S, Gao S, et al. Immune suppression in the early stage of
644 COVID-19 disease. *Nat Commun*. 2020;11. doi:10.1038/s41467-020-19706-9
- 645 43. Fulzele S, Sahay B, Yusufu I, Lee TJ, Sharma A, Kolhe R, et al. COVID-19 Virulence in Aged Patients
646 Might Be Impacted by the Host Cellular MicroRNAs Abundance/Profile. *Aging Dis*. 2020;11: 509–522.
647 doi:10.14336/AD.2020.0428
- 648 44. Tang Y, Liu J, Zhang D, Xu Z, Ji J, Wen C. Cytokine Storm in COVID-19: The Current Evidence and
649 Treatment Strategies. *Front Immunol*. 2020;11: 1708. doi:10.3389/fimmu.2020.01708
- 650 45. Tjan LH, Furukawa K, Nagano T, Kiriu T, Nishimura M, Arie J, et al. Early Differences in Cytokine
651 Production by Severity of Coronavirus Disease 2019. *J Infect Dis*. 2021;223: 1145–1149.
652 doi:10.1093/infdis/jiab005
- 653 46. Coperchini F, Chiovato L, Ricci G, Croce L, Magri F, Rotondi M. The cytokine storm in COVID-19:
654 Further advances in our understanding the role of specific chemokines involved. *Cytokine Growth Factor*
655 *Rev*. 2021;58: 82–91. doi:10.1016/j.cytogfr.2020.12.005
- 656 47. Cui J, Chen Y, Wang HY, Wang R-F. Mechanisms and pathways of innate immune activation and
657 regulation in health and cancer. *Hum Vaccines Immunother*. 2014;10: 3270–3285.
658 doi:10.4161/21645515.2014.979640
- 659 48. Takeda K, Kaisho T, Akira S. Toll-Like Receptors. *Annu Rev Immunol*. 2003;21: 335–376.
660 doi:10.1146/annurev.immunol.21.120601.141126

- 661 49. Sahanic S, Hilbe R, Dünser C, Tymozuk P, Löffler-Ragg J, Rieder D, et al. SARS-CoV-2 activates
662 the TLR4/MyD88 pathway in human macrophages: A possible correlation with strong pro-inflammatory
663 responses in severe COVID-19. *Heliyon*. 2023;9: e21893. doi:10.1016/j.heliyon.2023.e21893
- 664 50. Ziegler CGK, Allon SJ, Nyquist SK, Mbanjo IM, Miao VN, Tzouanas CN, et al. SARS-CoV-2 Receptor
665 ACE2 Is an Interferon-Stimulated Gene in Human Airway Epithelial Cells and Is Detected in Specific Cell
666 Subsets across Tissues. *Cell*. 2020;181: 1016-1035.e19. doi:10.1016/j.cell.2020.04.035
- 667 51. Wang L, Wang S, Li W. RSeQC: quality control of RNA-seq experiments. *Bioinforma Oxf Engl*.
668 2012;28: 2184–2185. doi:10.1093/bioinformatics/bts356
- 669 52. Dobin A, Davis CA, Schlesinger F, Drenkow J, Zaleski C, Jha S, et al. STAR: ultrafast universal RNA-
670 seq aligner. *Bioinforma Oxf Engl*. 2013;29: 15–21. doi:10.1093/bioinformatics/bts635
- 671 53. McMurdie PJ, Holmes S. phyloseq: An R Package for Reproducible Interactive Analysis and
672 Graphics of Microbiome Census Data. Watson M, editor. *PLoS ONE*. 2013;8: e61217.
673 doi:10.1371/journal.pone.0061217
- 674 54. Oksane J, Kindt R, Legendre P, O’Hara B, Simpson GL, Solymos P, et al. The vegan package.
675 *Community ecology package*. 2007;10: 631–637.
- 676 55. Kassambara A. ggpubr: “ggplot2” Based Publication Ready Plots. 2025. Available:
677 <https://rpkgs.datanovia.com/ggpubr/>
- 678 56. Kalantar KL, Carvalho T, De Bourcy CFA, Dimitrov B, Dingle G, Egger R, et al. IDseq—An open
679 source cloud-based pipeline and analysis service for metagenomic pathogen detection and monitoring.
680 *GigaScience*. 2020;9. doi:10.1093/gigascience/giaa111
- 681 57. Gu Z, Gu L, Eils R, Schlesner M, Brors B. circlize Implements and enhances circular visualization in
682 R. *Bioinforma Oxf Engl*. 2014;30: 2811–2812. doi:10.1093/bioinformatics/btu393
- 683 58. Love MI, Huber W, Anders S. Moderated estimation of fold change and dispersion for RNA-seq
684 data with DESeq2. *Genome Biol*. 2014;15: 550. doi:10.1186/s13059-014-0550-8
- 685 59. Luo W, Brouwer C. Pathview: an R/Bioconductor package for pathway-based data integration
686 and visualization. *Bioinforma Oxf Engl*. 2013;29: 1830–1831. doi:10.1093/bioinformatics/btt285
- 687
- 688